A Slip-Link Model of Branch-Point Motion in Entangled Polymers

S. Shanbhag and R. G. Larson*

Department of Chemical Engineering, University of Michigan, Ann Arbor, Michigan 48109-2136

Received April 24, 2003; Revised Manuscript Received August 11, 2004

ABSTRACT: In melts of asymmetric three-arm star polymers in which a short arm is attached to two long, equal-length arms, the existing "tube" theory fails to predict how rapidly the motion of the branch-point becomes quenched when the length of the third, short, arm grows from zero length, for which the two other arms form a reptating linear chain, to a length equal to the other two arms, for which reptation is quenched. We use a simulation method that represents entanglements between two chains as "slip-links" that allow local relaxation of both chains when an end of either chain passes through the slip-link. We include an extreme form of branch-point motion in this algorithm and find that it can explain the anomalously rapid quenching of the branch-point if we assume that the time scale of the branch-point motion is set by the time required for the short arm to escape all entanglements, including those newly created while others are destroyed. The algorithm successfully predicts the linear viscoelasticity of H-polymers, where the acceleration induced by the polydispersity offsets the sluggishness introduced by adopting a drastically slow time scale for diffusion of the branch-point. Although the theory becomes unrealistic for long arms, it raises important questions about existing theories of branch-point motion and provides some clues to their resolution.

Introduction

Significant progress has recently been made toward a more quantitative understanding of the linear viscoelasticity of linear and star polymer melts[1−3] using a model in which entanglements with surrounding chains create an effective "tube" within which the motion of a given test chain is confined. Upon application of a small "step" deformation, the relaxation dynamics of linear chains are modeled by considering the simultaneous action of three principal modes of stress relaxation, namely reptation, primitive-path fluctuations, and constraint release, yielding the well-known $\tau \sim M^{3.4}$ dependence of the largest relaxation time τ on molecular weight M. Stars, on the other hand, cannot reptate because they are "pinned" down by their branch-points. They relax only by the much slower processes of primitive path fluctuations and constraint release and their terminal relaxation times scale as $\tau \sim \exp(kM)$, where k is a constant.

Now consider growing a short arm from the center of a linear chain to obtain a three-armed asymmetric star. As the length of the short arm is increased gradually, we transform the linear polymer to a symmetric star. Intuitively, we would expect a gradual transition from the relatively fast dynamics that characterize linear chains to the slower dynamics of symmetric stars, as the length of the short arm is increased. Surprisingly, however, rheological data[4,5] show that the transition to "starlike" behavior sets in more quickly than anticipated, and most of the difference in rheological properties between linears and symmetric stars is already achieved in the asymmetric star when the short arm is only a small fraction of the length of the larger arms. Existing analytical theories[5] fail to predict this behavior, and the discrepancy is particularly severe when the asymmetric arm is relatively short.

It is speculated that the physics of branch-point motion, which is not very clearly understood, is the primary source the disagreement between experiment and theory. Recently, entanglements between two chains have been modeled as "slip-links" that act as constraints on both chains that are destroyed when either chain escapes the slip-link by reptation or primitive path fluctuations.[6−8] Proposals for branch-point motion can be examined with these slip-link models as will be demonstrated in this paper.

Current Analytical Theory

Frischknecht et al.[5] proposed a theory for the complex viscoelastic modulus $G^*(\omega)$ of a melt of asymmetric stars using the tube model. In their theory, following a small step strain, at a time equal to the Rouse time of an entanglement, τ_e, the arms "realize" that they are confined in tubes, and begin relaxing stress by primitive-path fluctuations.[9,10] There are two arm retraction times $\tau_l(s_l)$ and $\tau_s(s_s)$, corresponding to the relaxation times of a small segment of the long and short arms, respectively, both of which are functions of the fractional distances s_l and s_s along the long and short arms, respectively. The relaxed portions of long and short arms are treated as "solvent" for the remaining unrelaxed arm material. Once the short arm is completely relaxed at time $\tau_s^* = \tau_s(s_s = 1)$, the remaining unrelaxed long arms continue to retract in tubes dilated by this "solvent". Eventually, further relaxation by primitive-path fluctuations becomes very slow, and the long arms then continue their relaxation by reptation, with the asymmetric arm acting merely as a frictional drag element that controls the diffusivity of the branch-point D_b via

$$D_b = \frac{(pa_h)^2}{2\tau_s^*} \tag{1}$$

where a_h is the hopping distance of the branch-point and p is a dimensionless constant presumably of order unity. The total curvilinear diffusion constant, D_{eff}, of the long arms is then given by

$$\frac{1}{D_{eff}} = \frac{1}{D_b} + \frac{1}{D_c} \tag{2}$$

10.1021/ma034532m CCC: $27.50
Published on Web 09/23/2004

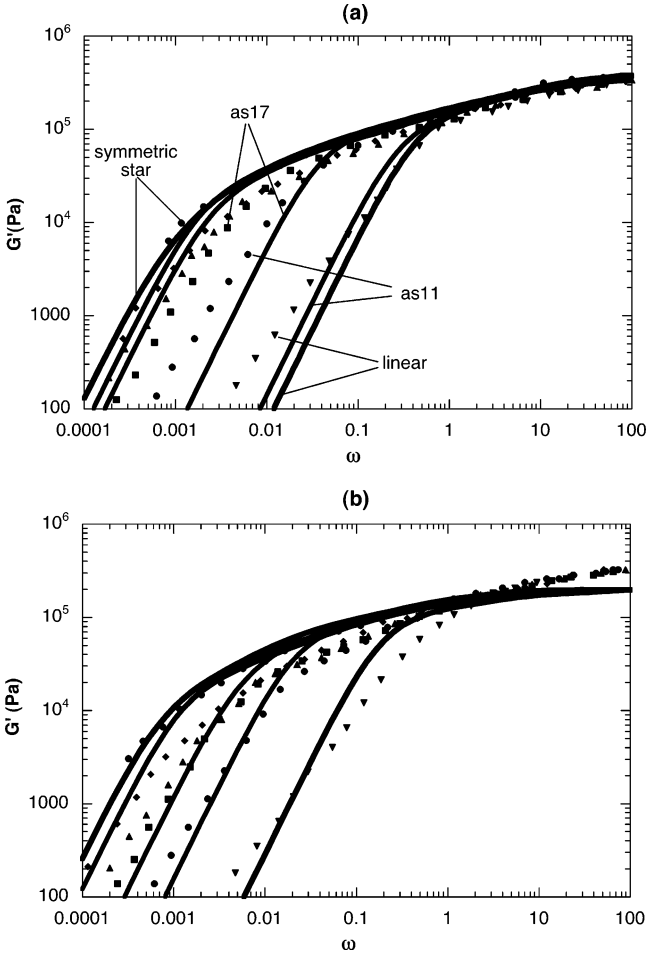

Figure 1. (a) Comparison of G' (storage modulus) predicted by analytical theory (ref 5) with experimental data. The predictions from the theory correspond to reptation and branch-point hops in a "skinny tube", and $p^2 = 1$, for melts of polyisoprene, in which the long ams are of molecular weight 105 000 and the short arms are of molecular weight (from right to left) 11 000 (circles), 17 000 (boxes), 37 000 (triangles), and 47 000 (diamonds), and the linear chain is of molecular weight $2 \times 105\,000$ ($M_e = 4650$). Note the large discrepancy between theory and experiment for short arms of molecular weight 11 000 and 17 000. (b) Comparison of G' predictions of sip-link simulations with the same experimental data. The simulation curves for asymmetric stars with short-arm molecular weights 37 000 and 47 000 are almost on top of each other. The parameters used in the simulation are $M_e = 4650$, $G_N^0 = 0.25$ MPa, and $\tau_0 = 1/42$ s.

where D_c is the Rouse diffusion constant of the "linear backbone", i.e., the two long arms. D_b decreases exponentially with the length of the short arm and for long short arms is expected to offer most of the resistance to curvilinear diffusion.

A comparison[5] of the theory with the experiment (Figure 1a) indicates that for asymmetric polyisoprene arms with short sidearms [samples as11, as17] the deviation between the above theory and experimental data for asymmetric polyisoprene star polymer melts is severe. The theory predicts a rate of relaxation that is much faster than observed in experiments.

The theory presented is a generalization of the "dynamic tube dilution" theory for symmetric stars with essentially two new elements. The first is the calculation of the drag associated with the branch-point given through eq 1. The second concerns with the question of whether reptation steps and branch-point hops take place in a "skinny" undilated tube or in a "fat" dilated tube. The failure (shown in Figure 1a) of the theory to predict the data is almost equally dramatic whether the reptation is in a "skinny" or "fat" tube. Also, while the failure for short asymmetric star arms can be "fixed" by arbitrarily choosing p^2 to be very small ($p^2 \approx 1/40$), such a small value seems physically unwarranted and leads to significant deviations in the predictions for the relaxation of polymers with longer asymmetric arms.

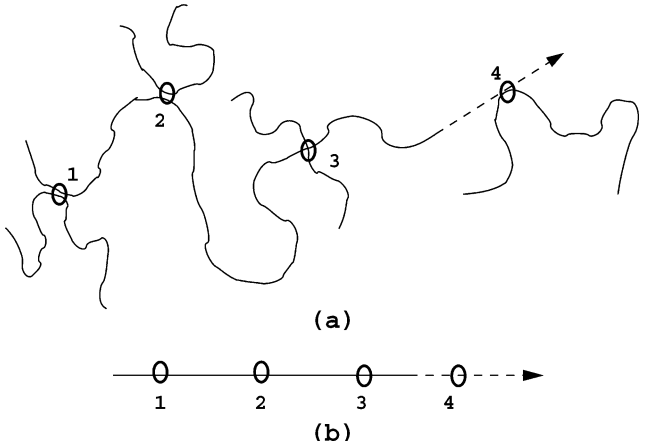

Figure 2. (a) Physical representation of a new slip-link being forged between chains i and j when the end of chain i hops outward. (b) Schematic representation in the slip-link model of the process in (a).

Dual Slip-Link Model

To address this problem, we turn to the dual slip-link model,[7] which has been used successfully to predict the viscoelastic and dielectric properties of symmetric star melts and to elaborate on some limitations of the dynamic dilution theory at long times. In this model, a physical entanglement between two chains is represented by a "slip-link", which locally restricts both chains until a free end of either one chain or the other slides through the slip-link, destroying it. It is not a real-space model; instead, it considers an ensemble of chains that are virtually coupled in that a point on chain i is linked to a point on chain j. When chain i releases the slip-link, this slip-link is also released from chain j. The equilibrium number of slip-links on an arm, Z_0, is equal to the average number of entanglements per arm, so that $Z_0 = M_a/M_e$, where M_a is the arm molecular weight and M_e the entanglement molecular weight ($M_e = 4650$ for polyisoprene[5]). The slip-link model is a coarse-grained description in which the smallest length scale is a, the undilated tube diameter. In the simulation, we permit the chain ends to fluctuate "outward" to create a fresh entanglement or to retract "inward" to destroy the entanglement (Figure 2). We use a Metropolis algorithm in which creation and destruction steps are attempted with equal probability, and their success is governed by a quadratic potential that mimics the well-known fluctuation potential of branched polymers[9]

$$U = \frac{\nu}{Z_0}(Z - Z_0)^2 \tag{3}$$

where Z is the instantaneous number of slip-links on the chain and $\nu = {}^3/_2$ is a factor that arises from the tube model. It may be noted that eq 3 has been a subject of debate. Lattice-based models[11,12] call into question the ability of a single equation like (3) to capture both

shallow and deep retractions and the applicability of a quadratic potential for deep fluctuations. We acknowledge that these issues are not yet resolved. However, we will continue to use eq 3 in the absence of a clear alternative.

To obtain the stress and dielectric relaxation functions from the relative ordering of slip-links, we assume that the slip-links are fixed in space and are separated from successive slip-links by an average distance of the tube diameter, a.

As described earlier,[7] the dielectric relaxation function, $\psi(t)$, depends on the relaxation of the end-to-end vector

$$\psi(t) = \frac{\langle \mathbf{R}(t)\cdot\mathbf{R}(0)\rangle}{\langle R^2\rangle} \tag{4}$$

where $\mathbf{R}(t)$ is the end-to-end vector of a chain and $\langle ...\rangle$ is the ensemble average. To calculate the contribution of a particular chain i to the dielectric relaxation function at any time in the slip-link model, we first identify the surviving slip-link on chain i that is farthest from the branch-point. Suppose that "p" denotes that a slip-link is the pth slip-link from the branch-point. For chain i at time t, this index, for the slip-link farthest from the branch-point that survives from time $t = 0$ to $t = t$, is denoted by $p_{f,i}(t)$. Then the contribution of chain i is given by

$$\psi_i(t) = \frac{p_{f,i}(t)}{p_{f,i}(0)} \tag{5}$$

This function captures the fraction of the original end-to-end vector of chain i that is still preserved.

The stress relaxation function, $\phi(t) = \sigma(t)/\sigma(0)$, can be relaxed whenever internal portions of the chain lose their alignment. For Gaussian chains

$$\sigma(t) = \sum_i \sum_s \left\langle \frac{\mathbf{R}^i_{s,s+1}\cdot\mathbf{R}^i_{s,s+1}}{N^i_s} \right\rangle \tag{6}$$

where $\mathbf{R}^i_{s,s+1}$ is the vector connecting closest neighboring original slip-links s and $s + 1$, that remain along the chain i at time t, with the branch-point counting as an original slip-link. N^i_s is the number of monomers in the portion of the chain between the two slip-links spanned by the vector $\mathbf{R}_{s,s+1}$.

Stress is thus proportional to the number of surviving slip-links. We compute the contribution of a particular chain i to the stress relaxation function by

$$\phi_i(t) = \frac{n_i(t)}{n_i(0)} \tag{7}$$

where $n_i(t)$ is the number of original slip-links surviving on chain i at time t. It may be noted that $p_{f,i}(t = 0) = n_i(t = 0)$.

In the case of monodisperse symmetric stars, the dual slip-link model, as mentioned earlier, has been successfully used to probe late-time behavior. Recent simulations (see Figure 3) on long PI stars have demonstrated the ability of the slip-link model to capture the hump in dielectric loss $\epsilon''/\Delta\epsilon$ reported in ref 13.

To account for the branch-point motion in asymmetric stars, we here modify the original dual slip-link model.

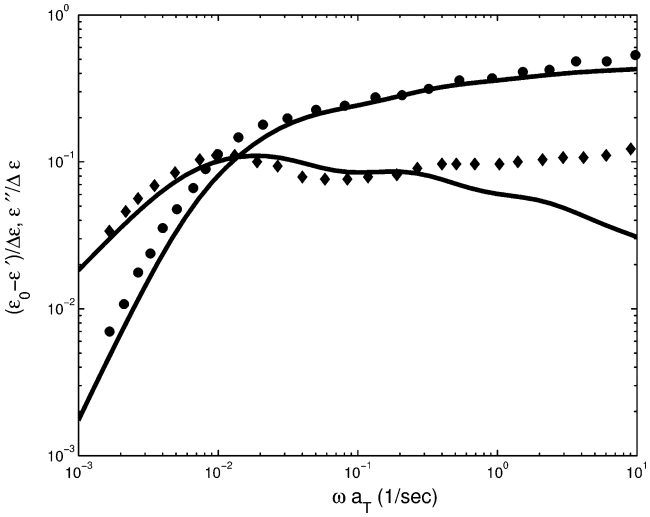

Figure 3. Normalized dielectric constant (filled circles) and dielectric loss constant (filled diamonds) at 40 °C for a 6-arm PI star with $M_w = 459\,000$. Symbols are data (ref 42), and lines are predictions using the slip-link model. The parameters of the model, $M_e = 4650$ and $\tau_0 = 1/42$ s, are the same as those used in ref 7 to predict the relaxation behavior of a polyisoprene star of lower molecular weight.

Since the short sidearm fluctuates more rapidly than the longer backbone arms, owing to its smaller drag, in the new simulation, we set the relative probabilities of choosing a sidearm versus a long arm for an attempted fluctuation step as

$$\frac{\text{prob}_s}{\text{prob}_l} = \left(\frac{Z_l}{Z_s}\right)^{1.5} \tag{8}$$

where Z is the number of entanglements and the subscripts s and l refer to the short and long arms. The power law of 1.5 was derived from the dependence of the prefactor for the exponential dependence of terminal relaxation time on molecular weight of symmetric stars in a fixed network (see Appendix A).

Further, we propose that each time the short arm retracts completely the branch-point can attempt a hop along the backbone. The direction of the hop ("right" or "left") is chosen randomly, and we restrict the hopping distance to one slip-link ($a_h = a$). For example, if the branch-point hops to the "left", we consider the move $Z_r = Z_r + 1$; $Z_l = Z_l - 1$, where Z_r and Z_l are the arm lengths of the two arms that make up the backbone of the asymmetric star. The success of the attempt is governed by the same potential given in eq 3.

The dual slip-link algorithm used for asymmetric stars may be summarized as follows:

1. Choose at random the end of some chain i for creation or destruction of a slip-link (based on the weighting scheme described above for short and long arms).

2. Choose between creation and destruction with equal probability.

3. If slip-link on the end of chain i is to be destroyed, find the partner chain j to which that slip-link is wedded. If the slip-link is to be added, choose a partner chain randomly and choose a random insertion position among the slip-links of chain j.

4. Compute change in combined potential of the two chains, $\Delta U_i + \Delta U_j$.

5. If $\Delta U_i + \Delta U_j < 0$, the move is accepted. If $\Delta U_i + \Delta U_j > 0$, accept the move with probability given by the Boltzmann factor, $\exp[-(\Delta U_i + \Delta U_j)]$.

6. If a destruction move has been accepted, check whether chain *i* or chain *j* has lost all its entanglements. If so, attempt a branch-point move as described above.

7. Return to step 1.

We use 300 molecules in our simulations and compute the stress relaxation function and the dynamic moduli by the method outlined in Shanbhag et al.[7] There is an adjustable parameter, τ_0, which sets the time scale of the simulation step, which is the same for simulations of all architectures of that particular chemical species (here, 1,4-polyisoprene). We also set the scale of stress through the plateau modulus, G_N^0, which we take to be $G_N^0 = 0.25$ MPa.

Results

Our modification to the original dual slip-link model to account for branch-point motion does not affect the relaxation dynamics of symmetric stars because the time scale on which an arm collapses and triggers an attempted branch-point hop is not smaller (is in fact significantly larger, as will be demonstrated later) than the terminal relaxation time, and branch-point motion thus becomes dynamically unimportant. An example of the success of the model for symmetric stars is given in Figure 3; an additional example is given in ref 7.

Next, we compare our simulation results for 300 molecules with the experimental data for asymmetric polyisoprene stars from ref 5. The results are insensitive to an increase in the number of molecules. We find that the collapse times, especially of the asymmetric stars with short sidearms, are much smaller than the terminal relaxation times of the molecule. The resultant mobility of the branch-point permits the asymmetric star to relax much faster than if the branch-point had been immobile. This is borne out in our simulations. Figure 1b shows that the storage moduli predicted by the simulations are in good agreement with the data and that the relaxation of the asymmetric stars with short sidearms (as11, as17) seems to have slowed down considerably as compared to the predictions of ref 5 in Figure 1a.

In the slip-link model, the hopping distance of the branch-point and the reptation step length are both considered to be equal to the distance between slip-links, which is equal to *a*, the entanglement spacing. This is equivalent to the assumption that reptation and the branch-point hops take place in a "skinny" or undilated tube, which, as we noted earlier, does not, by itself, lead to agreement of the analytic theory[5] with experimental data. Thus, at first glance, it may appear that the physical picture described by the slip-link model is equivalent to that described in ref 5 if the "skinny" tube is used. It may be recalled that comparisons between the dual slip-link model and the dynamic tube dilution (DTD) predictions for symmetric star melts[7] indicate that, except in the late-time region, the viscoelastic responses predicted by the slip-link model and the DTD theory are identical over a large frequency range.

The difference in the case of the asymmetric star, however, is in the treatment of the motion of the branch-point. We find that in the simulations the average time τ_s^* at which the short arm completely collapses is much larger than in the theory of Frischknecht et al.[5] The reason is illustrated in Figure 4a,b. In both cases (a) and (b), the tip of the star arm has "collapsed" to the branch-point, forming large entropically unfavorable loops. In Figure 4a, however, these loops have reentangled with some matrix chains, while in Figure 4b, the loops are free of all entanglements, both the original slip-links, and any new ones added after the step strain.

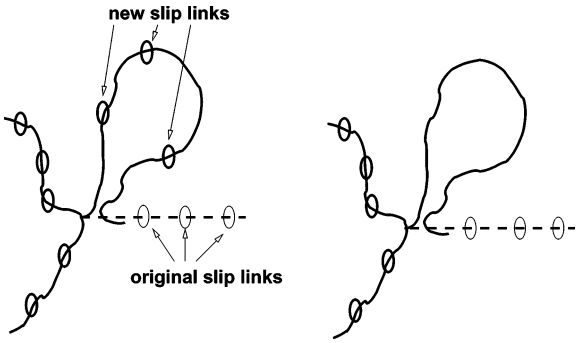

Figure 4. Physical situations corresponding to (a) first-passage time and (b) complete retraction, within the framework of the slip-link model. In both (a) and (b) the asymmetric arm has escaped all its original slip-links, but in (a) new slip-links have simultaneously been created by the motion of surrounding chains, while in (b) these new slip-links have also disappeared.

The tube model presented in ref 5 is not capable of distinguishing between the two cases depicted in Figure 4a,b, while the slip-link model can. The time corresponding to the "first-passage" problem in Figure 4a, τ_{fp}, can be obtained by calculating the average time required for the arm to lose all its "original" slip-links. The time corresponding to the "complete retraction" problem in Figure 4b, τ_{ret}, may be calculated by evaluating the average time it takes for the arm to lose all its slip-links.

We used the slip-link model to obtain τ_{fp} and τ_{ret} and indeed found that τ_{fp} was in reasonable agreement with the τ_s^* obtained from the analytical theory, although there were notable differences when $Z_{asym} < 6$. We argue that if an arm is entangled (or reentangled), it cannot be dragged along when the branch-point attempts a hop, and one ought to use $\tau_s^* = \tau_{ret}$ as the time step that sets the pace for the diffusion of the branch-point, as we did in our calculations.

Our simulation method implies a very strong dependence on the molecular weight of the arm that triggers branch-point hops. To test the validity of the algorithm independently, we simulated the linear viscoelastic response of 1,4-polyisoprene H-polymers [samples H110B20A and H160B40A] described in ref 14, which have average arm molecular weights of 20 000 and 40 000, corrsponding to 4.3 and 8.6 entanglements per arm, respectively. Since sample H160B40A was polydisperse (M_w/M_n was 1.05 in the arm and 1.30 in the backbone), we used the chemically characterized polydispersities in the arm and backbone molecular weights to create a corresponding distribution of equilibrium number of slip-links Z_0 in the simulations. The simulations are again for 1,4-polyisoprene, and so we use the same value of the time-step parameter determined from the data for stars; the results are shown in Figure 5a,b. We find that the relaxation dynamics of H-polymers are greatly accelerated by polydispersity, especially in the arms. This may be understood by noting that the terminal relaxation of H-polymers is governed by the relaxation of the backbone, which, in turn, is determined by the collapse time of the arms. Ignoring the Rouse

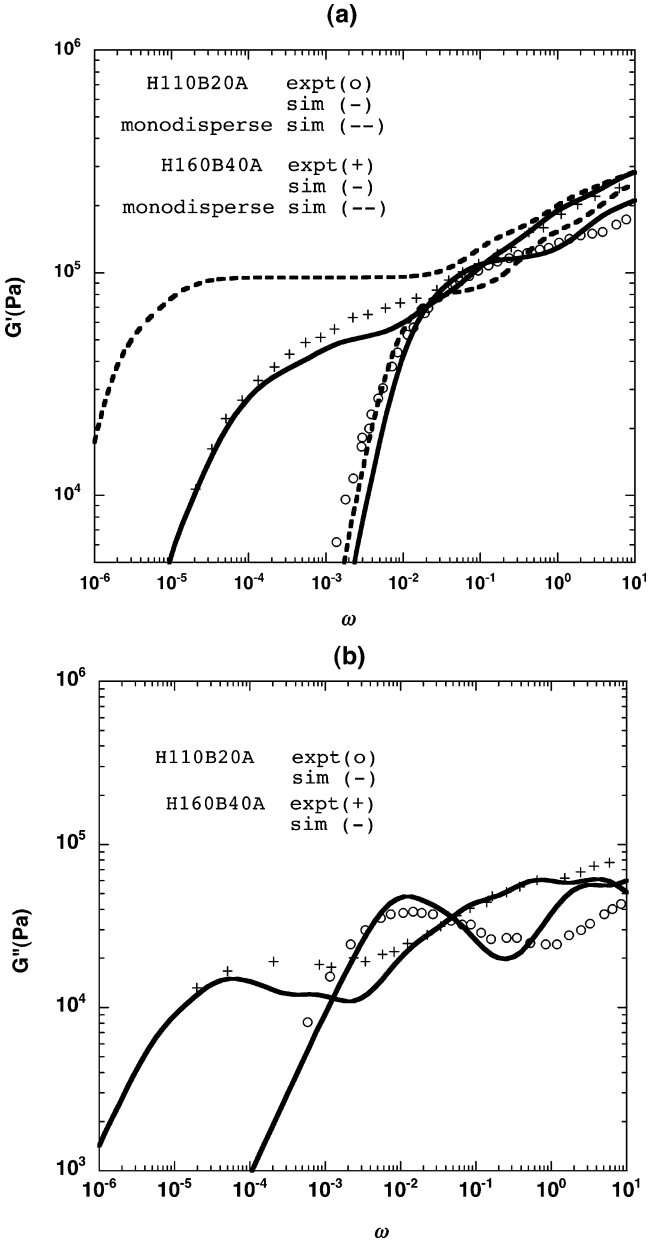

Figure 5. Comparison of (a) G' and (b) G'' of the slip-link model (lines) with no fitting parameters to experimental data (symbols) for polyisoprene H-polymers (ref 14) of total molecular weights 219 000 and 345 000, and arm molecular weights of 20 000 and 40 000, for samples H110B20A ($M_{w,arm}/M_{n,arm} = 1.01$, $M_{w,bb}/M_{n,bb} = 1.13$) and H160B40A ($M_{w,arm}/M_{n,arm} = 1.05$, $M_{w,bb}/M_{n,bb} = 1.30$), respectively. The dashed lines are the predicted results for monodisperse samples using the weight-averaged molecular weight.

diffusivity, the total curvilinear diffusivity of the backbone, $D_{eff,bb}$, may be approximated by

$$D_{eff,bb} \approx \frac{(pa_h)^2}{2}\sum_{i=1}^{4}\frac{1}{\tau^*_{s,i}} \qquad (9)$$

where i is an index that accounts for the four arms. From (9) it can be seen that $D_{eff,bb}$ is greatly increased if *any* one of the arms is short and is only moderately decreased by the presence of longer arms, since the rate of motion of the branch-point is set by the fastest relaxing arm(s). Therefore, in H-polymers, the sensitivity to the arm molecular weight can be counteracted by

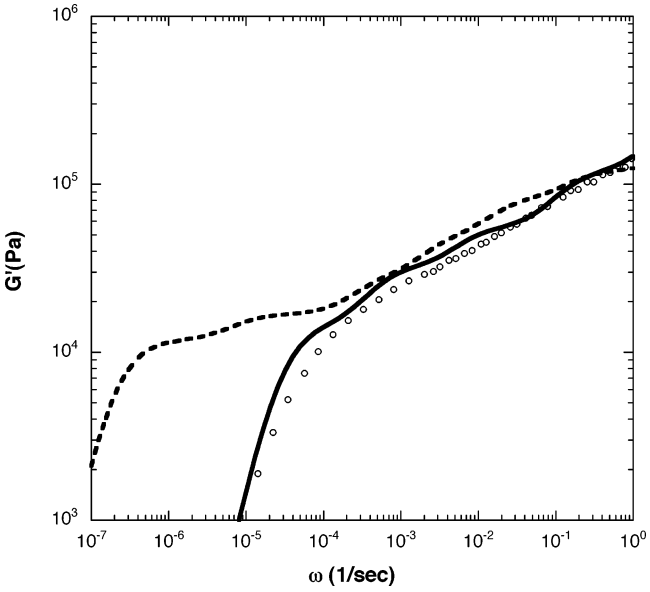

Figure 6. A comparison of G' predictions of the slip-link model (lines) to experimental data (symbols) for polyisoprene H-polymer (ref 14) sample H110A52 of total molecular weight 334 000, $M_{w,bb}/M_{n,bb} = 1.13$, and arm molecular weight of 52 500. The dashed line is the prediction for $M_{w,arm}/M_{n,arm} = 1.02$, and the thick line is when we adjusted arm polydispersity to be $M_{w,arm}/M_{n,arm} = 1.15$.

the sensitivity of the relaxation dynamics to polydispersity.

When we tried to simulate the H-polymer H110A52 using the reported values of polydispersity (M_w/M_n was 1.02 in the arm and 1.13 in the backbone), with arm molecular weight of 52 500, corresponding to 11.3 entanglements per arm, we found that there was an enormous discrepancy (about 2 orders of magnitude) between predictions and the data. The small reported polydispersity in the arm was insufficient to overcome the sluggishness introduced by the long arms. To bring the simulation and experiment into agreement, we had to adjust the polydispersity in the arm to $M_{w,arm}/M_{n,arm} = 1.15$ (see Figure 6). This is arbitrary, and at this point, we cannot justify having to use this large value. It may be pointed out that, so far, this is the only sample whose rheology has failed to be predicted by the slip-link algorithm. Other calculations on polystyrene H-polymers (included in Appendix B) and a preliminary calculation on a polyisoprene comb have also been successful.

Discussion

For asymmetric stars, the slip-link model succeeds where current analytical models fail. It invokes the idea of complete retraction, i.e., that an arm needs to lose all its slip-links before the branch-point can attempt a hop. The complete retraction time of an arm scales as the first passage time in a *fixed tube* and slows down the branch-point substantially. Thus, it implies that the self-diffusion constant of a symmetric star molecule would scale as $D \sim \exp(-1.5Z_a)$, which is drastically slower than $D \sim \exp(-0.59Z_a)$ observed in experiment.[16] Indeed, it seems untenable that a single slip-link far away from the branch-point can freeze the motion of the branch-point, indicating that the slip-link model is likely to fail as the arms get longer. The dual slip-link model is not a real-space model, and it is not possible to determine how far away from the branch-point the

slip-links are. As the arms get longer, the probability that the slip-link preventing the branch-point hop is far away from the branch-point is significant. The extreme failure of the model to simulate the H-polymer with the longest arms (H110A52) confirms this expectation. Empirically, we find that the slip-link model succeeds when the number of entanglements per arm is less than around eight and fails for arms longer than this. This result may be sensitive to polydispersity and other factors, however.

For three-arm hydrogenated polybutadienes Bartels et al.[16] report that the zero shear viscosity $\eta_0 \sim \exp(0.51Z_a)$ and $D \sim \exp(-0.59Z_a)$. When $D\eta_0$ is plotted against the number of entanglements on the arm, Z_a, an exponential decay is observed. This seems to suggest that the event which triggers a diffusive hop of the branch-point occurs less frequently than the event that marks the escape of an arm from the original tube. In current analytical models the two time scales are assumed to be the same, namely the first passage time in a dilated tube, while in the slip-link model the two time scales are assumed to be widely separated. Predictably, the analytical model fails in asymmetric arms when the asymmetric arm is short, and the slip-link model fails as the arm becomes longer when separation of the two time scales is widest.

It is possible to blame the simplicity of the dual slip-link model for overpredicting the collapse times of long arms. After all, it is not a real-space description and considers only a single mode of chain motion. There are other slip-link models in the literature[8,17] which offer a more detailed picture. This, however, comes at a price in terms of computation time and therefore in terms of the architectures that can be accessed. For example, the NAPLES code[8] performs a Brownian dynamics simulation of entangled polymers by solving a corresponding Langevin equation. To simulate a linear chain of $Z = 10$ entanglements, it takes about 2 h on a Xeon 3 GHz processor, and the simulation time is roughly proportional to the longest relaxation time. So, using a naive scaling analysis, it would take about 20 days to simulate a linear polymer with $Z = 50$ entanglements. To simulate a symmetric star with $Z = 22$ entanglements (i.e., the symmetric star from Frischknecht et al.[5]), it would take more than 7 months. Simulating more complex architectures such as H-polymers and combs with existing computer speeds is presently inconceivable. Even with parallelization or significant increase in processor speeds, probing diffusion in H-polymers is difficult. Although the slip-link model suffers from all the limitations that come from not being a real-space model, it nevertheless offers clues about branch-point motion; for example, it brings to light how the parallel structure implied by eq 9 could speed up the dynamics of H polymers with arm polydispersity. Despite the additional approximations involved, it is still worthwhile to explore structures that are currently inaccessible by more detailed slip-link models.

Conclusions

In summary, failure of conventional tube models to describe the linear viscoelastic data for asymmetric stars[5] prompted us to investigate the physics of branch-point motion more carefully. We found that it is important to define carefully what we mean by "collapse" of the small arm. The slip-link model is capable of distinguishing between "first passage" of the tip of the short arm all the way back to the branching point, $s = 1$, and "complete retraction", wherein the short arm loses all its entanglements, both "original" entanglements and newly created ones. While analytical models have assumed the former dictates the diffusion of the branch-point, we assumed the latter extreme in the slip-link model. It is able to describe not only the relaxation dynamics of symmetric and asymmetric stars but also those of more complex architectures, namely H-polymers. However, for reasons elaborated previously, the branch-point model suggested in the paper fails as the arm length increases. Our work suggests that two different time scales might govern the relaxation of polymer architectures in which branch-point motion is dynamically important and how the relaxation of the backbone in H-polymers might have to be modeled differently.

Acknowledgment. This material is based upon work supported by the National Science Foundation under Grant No. DMR 0072101. We also thank Dr. Seung Joon Park and Prof. Masubuchi at Nagoya University for helpful discussions.

Appendix A

The following is the general form for the terminal relaxation time of a star arm:

$$\tau(s{=}1) = \tau_0 Z^n \exp[U(s{=}1)] \tag{10}$$

where τ_0 is a time constant related to the so-called "equilibrium time",[15] and $U(s)$ is the fluctuation potential for arm retraction in a fixed matrix:

$$U(s) = \frac{3}{2}Zs^2 \tag{11}$$

To obtain $\tau(s{=}1)$ independently, we solve the problem of diffusion over a barrier, by numerically integrating the following equation:[18]

$$\tau(s{=}1) = (L^2/D)\int_0^1 ds' \exp[U(s')] \int_{-\infty}^{s'} ds'' \exp[-U(s'')] \tag{12}$$

where L is the contour length and D is the curvilinear diffusion constant of the retracting arm in the tube.

If we use these computed values of $\tau(s{=}1)$ from a numerical solution of eq 12 to fit the exponent n in eq 10, for $Z = 3-30$, we obtain $n = 1.46$, which justifies our choice of the power law in (8), for the relative relaxation probabilities.

Appendix B

We also tested the slip-link model on polystyrene H-polymers. We followed the same procedure used in predicting polyisoprene H-polymers mentioned earlier in the paper. First, we chose parameters to fit symmetric polystyrene star data from Grassley and Roovers.[19] We chose stars HS-51A ($M_{w,arm} = 256$K) and S171A ($M_{w,arm} = 181$K) as they were the most entangled stars for which the dynamic moduli data were available. The values of the parameters were $M_e = 13\,300$, $G_N^0 = 0.2$ MPa,[20] and $\tau_0 = 8.33$ ms (fitted).

A comparison of the simulation results with sample H1A1A, a polystyrene H-polymer,[21] is shown in Figure 7. The other H-polymers mentioned in the paper are either not very well entangled or do not have data in

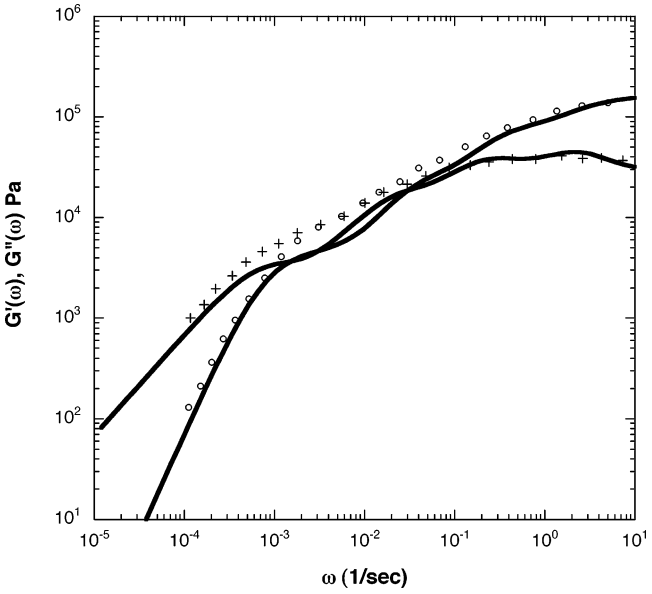

Figure 7. Comparison of G' (○) and G'' (+) predictions of the slip-link model (lines) with no fitting parameters to experimental data (symbols) for polystyrene H-polymer sample H1A1A (ref 21), assuming $M_{w,arm}/M_{n,arm} = 1.05$, $M_{w,bb}/M_{n,bb} = 1.05$. The molecular weights of the arm and backbone are 132 000 and 123 000, respectively.

the terminal region. In addition to the parameter τ_0 regressed from the comparison with symmetric stars, we used a "typical" polydispersity of $M_w/M_n = 1.05$ in both the arm and the backbone, since there was no polydispersity information in the paper. All the data mentioned in the literature are at 169.5 °C.

References and Notes

(1) Likhtman, A. E.; McLeish, T. C. B. *Macromolecules* **2002**, *35*, 6332−6343.

(2) Milner, S. T.; McLeish, T. C. B. *Macromolecules* **1997**, *30*, 2159−2166.

(3) Milner, S. T.; McLeish, T. C. B. *Macromolecules* **1998**, *31*, 7479−7482.

(4) Gell, C. B.; Graessley, W. W.; Efsratiadis, V.; Pitsikalis, M.; Hadjichristidis, N. *J. Polym. Sci., Part B* **1997**, *35*, 1943−1954.

(5) Frischknecht, A. L.; Milner, S. T.; Pryke, A.; Young, R. N.; Hawkins, R.; McLeish, T. C. B. *Macromolecules* **2002**, *35*, 4801−4819.

(6) Hua, C. C.; Schieber, J. D. *J. Chem. Phys.* **1998**, *109*, 10018−10027.

(7) Shanbhag, S.; Larson, R. G.; Takimoto, J.-I.; Doi, M. *Phys. Rev. Lett.* **2001**, *85*, 195502.

(8) Masubuchi, Y.; Takimoto, J.-I.; Koyama, K.; Ianniruberto, G.; Marrucci, G.; Greco, F. *J. Chem. Phys.* **2001**, *115*, 4387−4394.

(9) Pearson, D. S.; Helfand, E. *Macromolecules* **1984**, *17*, 888−895.

(10) Doi, M.; Kuzuu, N. Y. *J. Polym. Sci., Polym. Lett. Ed.* **1980**, *18*, 775−780.

(11) Rubinstein, M.; Helfand, E. *J. Chem. Phys.* **1985**, *82*, 4387−4394.

(12) Zheligovskaya, E. A.; Ternovskii, F. F.; Khokhlov, A. R. *Theor. Math. Phys.* **1988**, *75*, 644−653.

(13) Watanabe, H.; Matsumiya, Y.; Inoue, T. *Macromolecules* **2002**, *35*, 2339−2357.

(14) McLeish, T. C. B.; et al. *Macromolecules* **1999**, *32*, 6734−6758.

(15) Doi, M.; Edwards, S. F. *The Theory of Polymer Dynamics;* Clarendon Press: Oxford, 1986.

(16) Bartels, C. R.; et. al. *Macromolecules* **1986**, *19*, 785−793.

(17) Doi, M.; Takimoto, J.-I. *Philos. Trans. R. Soc. London, Ser. A: Math. Phys. Eng. Sci.* **2003**, *361*, 641−650.

(18) Risken, H. *The Fokker-Plank Equation;* Springer-Verlag: Berlin, 1989.

(19) Grassley, W. W.; Roovers, J. *Macromolecules* **1979**, *12*, 959−965.

(20) Fetters, L. J.; et. al. *Macromolecules* **1994**, *27*, 4639−4647.

(21) Roovers, J. *Macromolecules* **1984**, *17*, 1196−1200.

MA034532M